Editors' Suggestion

Fate of Quasiparticles at High Temperature in the Correlated Metal Sr_2RuO_4

A. Hunter,[1] S. Beck,[2] E. Cappelli,[1] F. Margot,[1] M. Straub,[1] Y. Alexanian,[1] G. Gatti,[1] M. D. Watson,[3] T. K. Kim,[3] C. Cacho,[3] N. C. Plumb,[4] M. Shi,[4] M. Radović,[4] D. A. Sokolov,[5] A. P. Mackenzie,[5,6] M. Zingl,[2] J. Mravlje,[7,8] A. Georges,[1,2,9,10] F. Baumberger,[1,4] and A. Tamai[1]

[1]*Department of Quantum Matter Physics, University of Geneva, 24 Quai Ernest-Ansermet, 1211 Geneva 4, Switzerland*
[2]*Center for Computational Quantum Physics, Flatiron Institute, 162 Fifth Avenue, New York, New York 10010, USA*
[3]*Diamond Light Source, Harwell Campus, Didcot, OX11 0DE, United Kingdom*
[4]*Swiss Light Source, Paul Scherrer Institut, CH-5232 Villigen PSI, Switzerland*
[5]*Max Planck Institute for Chemical Physics of Solids, 01187 Dresden, Germany*
[6]*Scottish Universities Physics Alliance, School of Physics and Astronomy, University of St. Andrews, St. Andrews KY16 9SS, United Kingdom*
[7]*Department of Theoretical Physics, Institute Jozef Stefan, Jamova 39, SI-1001 Ljubljana, Slovenia*
[8]*Faculty of Mathematics and Physics, University of Ljubljana, Jadranska 19, SI-1000 Ljubljana*
[9]*Collège de France, 11 Place Marcelin Berthelot, 75005 Paris, France*
[10]*Centre de Physique Théorique, Ecole Polytechnique, CNRS, Institut Polytechnique de Paris, 91128 Palaiseau Cedex, France*

(Received 4 August 2023; accepted 8 November 2023; published 8 December 2023)

We study the temperature evolution of quasiparticles in the correlated metal Sr_2RuO_4. Our angle resolved photoemission data show that quasiparticles persist up to temperatures above 200 K, far beyond the Fermi liquid regime. Extracting the quasiparticle self-energy, we demonstrate that the quasiparticle residue Z increases with increasing temperature. Quasiparticles eventually disappear on approaching the bad metal state of Sr_2RuO_4 not by losing weight but via excessive broadening from super-Planckian scattering. We further show that the Fermi surface of Sr_2RuO_4—defined as the loci where the spectral function peaks—deflates with increasing temperature. These findings are in semiquantitative agreement with dynamical mean field theory calculations.

DOI: 10.1103/PhysRevLett.131.236502

Many correlated electron systems with diverse magnetic and electronic ground states turn into bad metals at high temperature—that is, their resistivity increases with temperature and shows no sign of saturation well beyond the Mott-Ioffe-Regel (MIR) limit, where the mean free path defined in semiclassical transport models drops below interatomic distances [1–3]. Examples include cuprates [4], ruthenates [5], iron pnictides [6,7], manganites [8], alkali doped C_{60} [9], and organic salts [10].

A pragmatic definition of a quasiparticle (QP), adopted throughout this Letter, is the existence of a clearly discernible peak in the spectral function. The bad metal state at or beyond the MIR limit does not host quasiparticlelike excitations, because, with a coherence length below the Fermi wavelength, a particlelike description is no longer appropriate. This is qualitatively consistent with angle-resolved photoemission spectroscopy (ARPES) studies of cobaltates [11], ruthenates [12–14], or iron chalcogenides [15,16], which all found that QPs disappear at temperatures well below the MIR limit. This behavior was thus far interpreted as a gradually decreasing QP residue Z with increasing temperature [11,13]. A crossover where $Z \to 0$ with increasing temperature is also found in a slave boson [17] and in dynamical mean field theory (DMFT) [10,18,19] studies of the single-band Hubbard model for undoped systems close to the metal-insulator transition. Work on organic salts found that the transition $Z \to 0$ manifests itself as a crossover from a bad metal regime in which Z is finite to a semiconductorlike resistivity at high temperature where $Z \approx 0$ [10]. Such a resistive transition is reminiscent of the c-axis resistivity in Sr_2RuO_4 [20] but is not observed for in-plane transport in Sr_2RuO_4 and most other bad metals.

An alternative picture that is intuitively appealing for metallic systems is that at elevated temperatures excitations become more bare-electron-like and that QPs become short-lived but simultaneously lose renormalization such that $Z \to 1$. This behavior is indeed found in DMFT studies of the doped Hubbard model [21,22] and of Hund metals [23–25].

The QP residue Z is defined as $Z_k = (1 - \partial\Sigma'(\omega, k)/\partial\omega|_{\omega=0})^{-1}$, where Σ' is the real part of the self-energy. Z corresponds to the integral of the coherent QP peak in the spectral function and is, thus, also called QP weight. However, in real systems there is no established way to distinguish the "coherent" from the "incoherent" part of the spectrum, and, therefore, extracting Z from an analysis of spectral weight may be difficult. Moreover, in ARPES

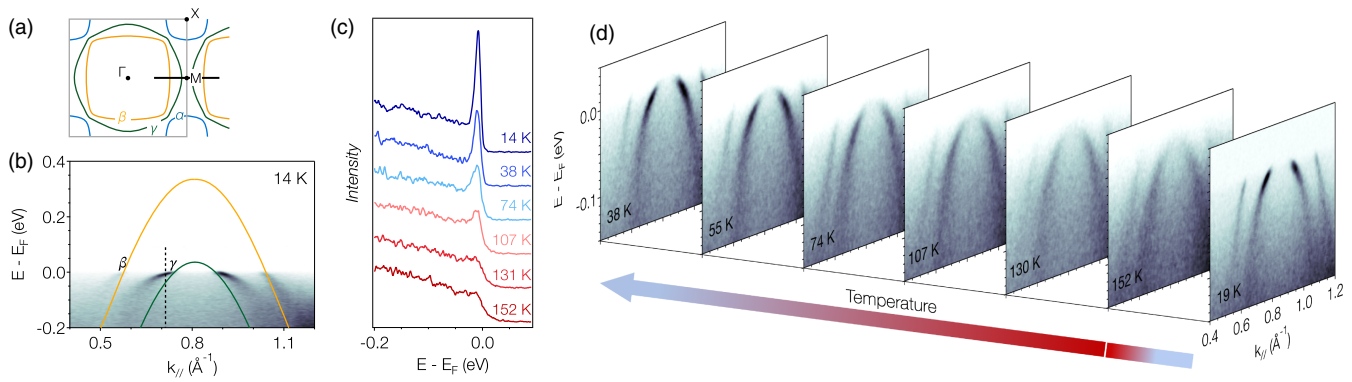

FIG. 1. (a) Schematic of the Fermi surface of Sr_2RuO_4. (b) Low-temperature ARPES data showing the β and γ band dispersing symmetrically around the Brillouin zone boundary. Yellow and green lines are the bare dispersions of the β and γ bands, respectively, obtained from the Hamiltonian introduced in Ref. [26]. (c) EDCs extracted for the γ band at the momentum indicated by a dashed line in (b), corresponding to a QP energy of -10 meV. (d) Temperature dependence of the ARPES spectral functions for the same cut shown in (b). Data are shown in reverse chronological order over a complete temperature cycle.

data, it is often not obvious how to separate increasingly broad peaks from the background which is often poorly understood.

Here, we address these issues by studying the fate of QPs in Sr_2RuO_4 with increasing temperature. Analyzing the dispersion measured by ARPES rather than the spectral weight, we show that the QP residue Z increases in Sr_2RuO_4 with increasing temperature, contrary to earlier reports. QPs eventually disappear at elevated temperature by "dissolving" in the incoherent part of the spectrum rather than by losing spectral weight. We further show that the evolution of Z with temperature derived from our data is in agreement with DMFT calculations and fully consistent with the ARPES spectral weight.

Sr_2RuO_4 is an ideal material to address the evolution of the QP residue Z with temperature. In its normal state, Sr_2RuO_4 is a prototypical correlated metal with a well-understood electronic structure, a large mass enhancement, and sharp QP peaks at low temperature [26–28]. Resistivity data show a well-defined Fermi liquid regime below $T_{\mathrm{FL}} \approx 25$ K crossing over to an extended regime with T-linear resistivity [5,29]. Depending on the precise criterion, the MIR limit is surpassed for $\rho = 0.1$–0.7 mΩ cm reached at $T = 300$–800 K [5]. Crucially for our approach here, the self-energy of Sr_2RuO_4 is dominated by local electron-electron correlations and, thus, does not have significant momentum dependence [26,30]. In this limit, the QP residue is related to the velocity renormalization $(v_F/v_{\mathrm{bare}}) = Z$, where v_F and v_{bare} are the QP and bare Fermi velocity, respectively. We will base our quantitative analysis on this relation (and refer to this quantity as "QP residue") before demonstrating that Z obtained in this way is fully consistent with the integral of coherent spectra (referred to as "QP weight").

Figure 1 shows ARPES data of Sr_2RuO_4 acquired at a photon energy of 40 eV. Details of the measurement conditions are given in Supplemental Material [31]. Throughout this Letter, we focus on the momentum space cut marked by a thick black line in Fig. 1(a). Along this high-symmetry line, orbital hybridization is minimal, and the β and γ sheets retain $\approx 80\%$ xz/yz and xy orbital character, respectively [26].

The comparison in Fig. 1(b) with the bare band dispersion introduced in Ref. [26] illustrates the strong and orbital-dependent mass enhancement of the QP excitations in Sr_2RuO_4 documented in the literature [26,27,47]. Intriguingly, monitoring the spectral function with increasing temperature reveals an apparent dichotomy between energy distribution curves (EDCs) and the two-dimensional energy-momentum images. The EDCs of the γ band [Fig. 1(c)] show a well-defined sharp peak at low temperature that decays with increasing temperature and appears to be swallowed by the background around 130 K. Similar observations in earlier work were interpreted as a transition $Z \to 0$ and have been related to the crossover to semiconducting c-axis transport in Sr_2RuO_4 [13,20]. Interestingly, though, the ARPES image plots in Fig. 1(d) show QP-like bands up to higher temperature with no sign of a transition at 130 K. Additional data in Supplemental Material (Fig. S9) [31] shows that bandlike states persist up to ≈ 250 K. This illustrates that analyzing spectral weights in EDCs is delicate and may not be robust. We note that the apparent suppression of peaks in EDCs is not an artifact of the Fermi cutoff. In Fig. 1(c), we deliberately extracted EDCs at an initial state energy of -10 meV to minimize effects of the Fermi-Dirac distribution.

We start our quantitative analysis by fitting the peak positions of the β and γ bands in momentum distribution curves (MDCs). Assuming that both bands disperse symmetrically around the Brillouin zone boundary, we obtain their Fermi wave vectors from $k_F^{\beta,\gamma} = \pi/a - \Delta k^{\beta,\gamma}/2$, where $\Delta k^{\beta,\gamma}$ is the separation of the Fermi level crossings in the first and second Brillouin zone, as indicated in

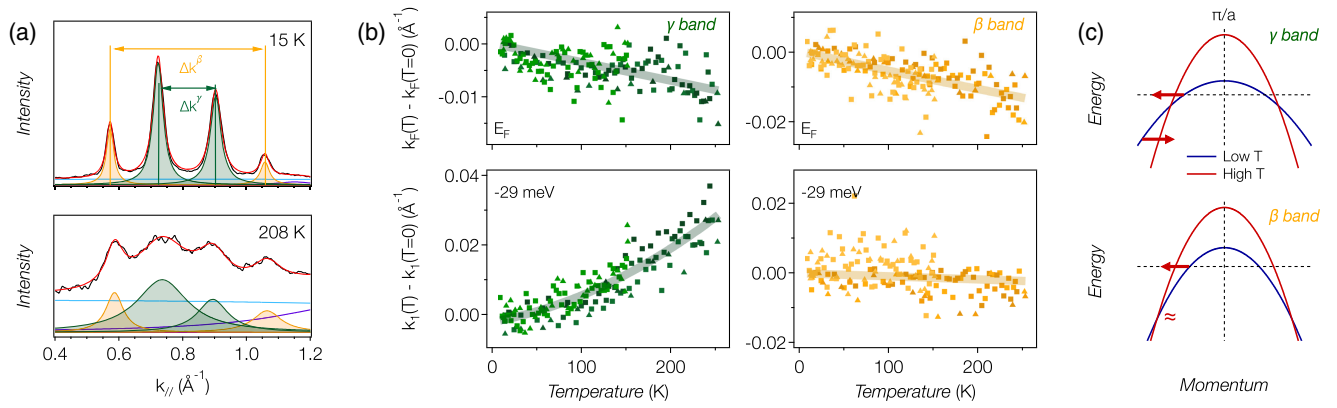

FIG. 2. (a) MDCs at E_F extracted from ARPES data with Lorentzian fits to quantify peak positions of the β and γ band. Additional examples of fits are shown in Supplemental Material, Fig. S5 [31]. (b) Temperature dependence of $k(T) - k(T = 0)$ at $E = E_F$ and $E = -29$ meV. Different colors indicate different experimental runs. Squares and triangles represent temperature up and down sweeps, respectively. The values shown have been corrected for finite energy resolution as described in Supplemental Material [31]. Raw peak positions from MDC fits are shown in Supplemental Fig. S7(c) [31]. (c) Schematic illustrating the temperature evolution of the QP dispersion of the β and γ band.

Fig. 2(a). We note that finite energy resolution leads to an "up turn" in the apparent dispersion measured by ARPES with peak positions in MDCs that deviate from the quasiparticle dispersion [48]. We have quantified this artifact (see Supplemental Material, Figs. S6 and S7 [31]) using DMFT spectral functions—which are known to provide a good description of high-resolution laser-ARPES data [26]—and show in Fig. 2(b) directly the corrected wave vectors. As a further cross-check, we performed 2D fits of the ARPES data that include resolution effects directly as a convolution with a 2D response function. The results from these 2D fits are fully consistent with the MDC analysis shown here (see Supplemental Material, Fig. S10 [31]).

Intriguingly, our analysis shows that k_F shrinks with increasing temperature for both bands. This signifies a deflation of both the β and γ sheets. Such a change in Fermi surface volume cannot arise from interorbital charge transfer; neither does it imply a reduction of the carrier density. Our DMFT calculations—in which the integral over the spectral function precisely reproduces the number of electrons—show a comparable deflation of the Fermi surfaces, as shown in Supplemental Material, Fig. S6 [31]. This appears to be a consequence of the van Hove singularity above E_F that tends to increase electron occupancy at high temperature when QPs broaden. This change must be compensated by diminishing $\mu - \Sigma'(\omega = 0)$ (here, μ is the chemical potential) in order to maintain the total electron count, which, in turn, leads to a reduced k_F and apparent deflation of the Fermi surface. However, this argumentation is not general. It assumes that the incoherent parts of the spectral function do not change importantly with temperature, which does not always hold [21,22,49]. Changes in Fermi surface volumes were also observed in iron pnictides [50,51], but there the behavior might have different contributions including magnetism, charge reorganization due to thermal expansion, and possibly also a partial localization of carriers.

Extending the analysis of MDCs to energies below the chemical potential shows a remarkable orbital differentiation. The QP band position k_1 at $E - E_F = -29$ meV increases markedly for the γ sheet, while it is nearly temperature independent for the β sheet. We have verified that this behavior cannot be attributed to the effects of thermal expansion on the bare band structure. Hence, we conclude that both QP bands "unrenormalize" with increasing temperature, but the γ sheet does so much more rapidly and in a slightly different way, as indicated pictorially in Fig. 2(c).

We estimate the QP residue Z from our analysis by assuming a parabolic dispersion of the β and γ bands symmetrically around the Brillouin zone boundary at π/a. In this case, the QP Fermi velocity $v_F(T)$ is uniquely determined by $k_F(T)$ and $k_1(T)$. Figure 3(a) shows $Z(T) = v_F(T)/v_{\text{bare}}$ obtained in this approximation for $v^{\beta}_{\text{bare}} = 2.57$ eV Å and $v^{\gamma}_{\text{bare}} = 1.06$ eV Å obtained from the bare Hamiltonian in Ref. [26]. We find that Z in Sr_2RuO_4 increases with temperature. For a direct comparison of our experimental results with DMFT calculations, we transform Z^{DMFT} from an orbital to a band basis, as described in Ref. [26] [dashed black lines in Fig. 3(a)]. This reproduces the slope of $Z(T)$ found in experiment. We note that the QP residues obtained from our MDC analysis are slightly higher than found in DMFT and in a previous ARPES study restricted to low temperatures [26]. This difference is reduced in a 2D analysis of the experimental data (see Supplemental Material [31]).

The temperature dependence of Z affects the QP scattering rate $\Gamma_{\text{QP}} = \hbar/\tau$. In Fig. 3(b), we compare Γ_{QP} obtained from 2D fits of the experimental data with DMFT and the Planckian

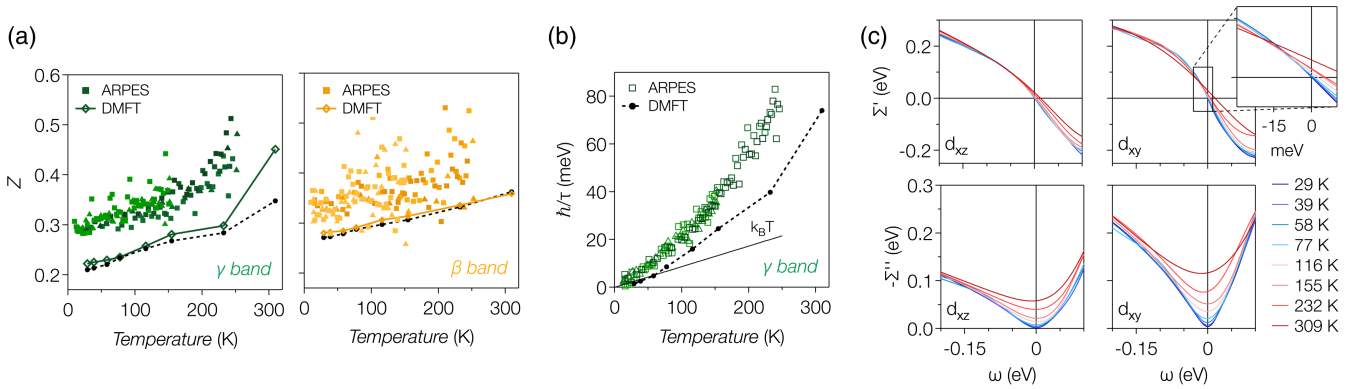

FIG. 3. (a) Temperature dependence of $Z = v_F/v_{\mathrm{bare}}$ for the γ and β bands compared to DMFT calculations. Filled symbols with different color shading indicate different experimental runs. Squares and triangles represent temperature up and down sweeps, respectively. The dashed black lines give $Z_\nu = \left(\sum Z_m^{-1}|U_{m\nu}(k)|^2\right)^{-1}$. Diamond symbols connected by lines are obtained by repeating the ARPES analysis on DMFT spectral functions. (b) QP line width $\Gamma_{\mathrm{QP}} = \hbar/\tau$ (full width half maximum) obtained from 2D fits compared with DMFT results and the Planckian limit $k_B T$. In (a) and (b), different symbols and colors are used for different experimental runs and temperature up and down sweeps. (c) DMFT self-energies.

value $k_B T$ [52,53]. We restrict this comparison to the γ band, for which the 2D fits are more reliable. The DMFT QP linewidth is calculated from $\Gamma_\nu = \sum \Gamma_m |U_{m\nu}(k)|^2$, where m and ν are the orbital and band indices, respectively, $\Gamma_m = -\Sigma''(\omega, T)\{1 - [\partial\Sigma'(\omega, T)/\partial\omega]|_\omega\}^{-1}$, and $|U_{m\nu}|^2$ is the orbital content obtained from the bare Hamiltonian. One sees that the scattering rate exceeds the Planckian bound already for $T \gtrsim 50$ K and continues to grow with a positive curvature. The scattering rates obtained from the ARPES data are in quantitative agreement with resistivity measurements (see Supplemental Material [31]). We further note that the slight underestimation of $\hbar/\tau$ in DMFT is fully consistent with the small contribution of electron-phonon scattering identified in recent theoretical work [54].

Figure 3(c) shows that the deflation of the Fermi surfaces of Sr_2RuO_4 and the "unrenormalization" of its QP dispersion reported here are readily discernible in the DMFT self-energies. The slope of Σ' reduces for both orbitals with increasing temperature, implying that the Fermi fluid in Sr_2RuO_4 is less renormalized at higher temperature. At the same time, $\Sigma'(T, \omega = 0)$ increases with temperature, causing a positive QP energy at the bare Fermi wave vector and, thus, a deflation of the Fermi surface.

We now return to the evolution of spectral weights with temperature. Our findings in Fig. 3 of Z which increases with temperature indicate that the QP spectral weight should also increase with temperature. However, this appears to be in contradiction with the temperature-dependent EDCs presented in Fig. 1(c), which show QP peaks gradually becoming swallowed by the background. Indeed, it is this picture of temperature-dependent EDCs which has led to previous conclusions of Z decreasing as temperature is increased [13]. This apparent discrepancy poses an important conceptual question: Are QP weights and velocity normalizations responding differently to a change in temperature? To answer this question, we first analyze QP weights in DMFT spectral functions.

Figure 4(a) shows DMFT spectra $A(k_0, \omega)$ calculated for a momentum k_0 where the QP energy of the γ band is ≈ -20 meV. The main peak just below the chemical potential can, thus, be attributed to the γ band. Additional peaks in the unoccupied states and around -0.4 eV originate from the β and α bands, respectively. As expected, the γ band QP peak broadens progressively with increasing temperature, and its height diminishes. At the same time, it evolves from the typical asymmetric Fermi liquid line shape at low temperatures toward a Lorentzian at elevated temperature.

To estimate the QP spectral weight, we expand the self-energy to first order around the QP peak position ω_0: $\Sigma' = \Sigma'_0 + (1 - 1/Z)\delta\omega$ and $\Sigma'' = \Sigma''_0 + \alpha\delta\omega$, where $\delta\omega = \omega - \omega_0$. The spectral function is then given by $A_1(k, \delta\omega) \approx -\pi^{-1} Z^2(\Sigma''_0 + \alpha\delta\omega)/[\delta\omega^2 + Z^2(\Sigma''_0 + \alpha\delta\omega)^2]$. Fits of the DMFT spectra with this expression show that the first-order approximation is sufficiently flexible to capture the evolution of the line shape with temperature and provides a physically meaningful estimate of the QP weight. Significantly, we find that the QP weight does increase with temperature despite the peaks becoming less intense. The direct comparison of the QP weight from these fits with $Z(\omega_0) = [1 - (\partial\Sigma'/\partial\omega)|_{\omega_0}]^{-1}$ obtained from the DMFT self-energy [inset in Fig. 4(a)] shows minor quantitative differences but illustrates that the concept of QP weight remains meaningful at elevated temperature in DMFT spectra of multiband systems.

We now address the consistency of ARPES spectral weights with the increase in Z found from the ARPES dispersions. To this end, we first isolate the intrinsic spectral function from the ARPES spectra by subtracting a "background." The latter arises from inelastically

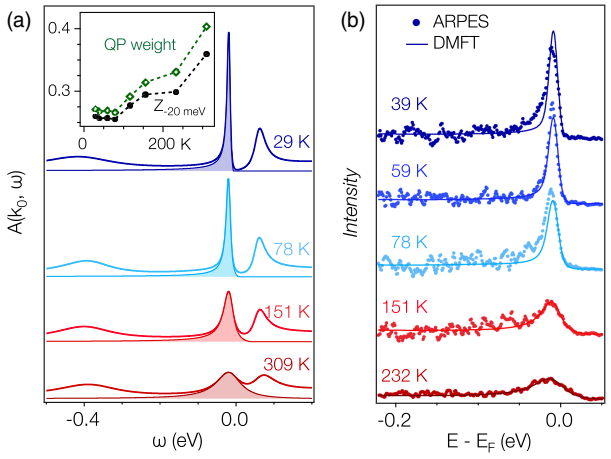

FIG. 4. (a) DMFT spectral functions calculated for a momentum where the QP energy of the γ band is ≈ -20 meV [near the dashed black line in Fig. 1(b)]. Shaded areas indicate the coherent QP spectral weight as identified by fits (see main text). The inset shows the temperature dependence of the QP weights (green) compared to $Z(\omega = -20\ \mathrm{meV})$ extracted from Σ' (black). (b) Background subtracted ARPES EDCs of the γ band QP at -10 meV compared to corresponding DMFT spectral functions multiplied by a Fermi function and convolved by a Gaussian to account for the experimental resolution.

scattered electrons but may also contain contributions from the interference of multiple photoemission channels and is notoriously hard to model [55,56]. We, therefore, resort to a pragmatic approach and approximate the background with the spectrum at π/a where no direct transitions are observed in the relevant energy range (see Supplemental Material, Sec. VIII [31], for more details). In contrast to the approach of Ref. [13], this results in spectra with QP-like excitations persisting up to the highest temperatures of $\approx$250 K studied in our experiment [Fig. 4(b)].

Direct fits of these background subtracted spectra with $A_1(k, \delta\omega)$ given above proved to be unstable. However, the evolution of the line shape and peak intensity in our experimental data is in excellent agreement with DMFT spectral functions as shown in Fig. 4(b). Note that in this comparison we apply only a global, temperature-independent scaling factor between the DMFT and the experimental spectra. This implies that the experimental spectral weights are fully consistent with an increase in Z with increasing temperature.

In summary, our work shows that QPs in Sr_2RuO_4 are resilient up to temperatures approaching the MIR limit. Notably, we find no abrupt changes in behavior as the temperature crosses $T_{FL} \approx 25$ K or through the metal-insulator crossover in ρ_c at $\approx$130 K. Quantitative analysis shows that the QP residue Z increases with increasing temperature. This resolves the inconsistency of previous experimental findings with modern numerical many-body calculations [13,23–25] and constrains theoretical descriptions of the bad metal state of Sr_2RuO_4. It also raises the question whether the behavior found here is the only one consistent with bad metal transport. Hund metals with an orbital selective Mott phase, as proposed by Yi *et al.* for certain iron chalcogenides [15], may show QP weights $\to 0$ for orbitals that localize, while the weights of orbitals contributing to high temperature transport may well show the behavior uncovered here for Sr_2RuO_4. An important issue for future experimental work will be to investigate QP residues in Mott systems such as VO_2 and V_2O_3 or doped iridates and cuprates [57,58].

The research data supporting this publication can be accessed at the Yareta repository of the University of Geneva [59].

We thank J. Schmalian and P. D. C. King for discussions. The ARPES work was supported by the Swiss National Science Foundation (SNSF), Grant No. 184998. We acknowledge Diamond Light Source for time on Beam line I05 under Proposal No. SI25083 and the Paul Scherrer Institut, Villigen, Switzerland for provision of synchrotron radiation beam time at the SIS beam line of the SLS. The Flatiron Institute is a division of the Simons Foundation. A. P. M. acknowledges the support of the Max Planck Society and the German Research Foundation (TRR288-422213477 ELASTO-Q-MAT, Project A10). Research in Dresden benefits from the environment provided by the DFG Cluster of Excellence (ct.qmat EXC 2147, Project No. 390858490). J. M. was funded by the Slovenian Research Agency (ARIS) under Project No. J1-2458.

[1] V. J. Emery and S. A. Kivelson, Superconductivity in bad metals, Phys. Rev. Lett. **74**, 3253 (1995).
[2] O. Gunnarsson, M. Calandra, and J. E. Han, Colloquium: Saturation of electrical resistivity, Rev. Mod. Phys. **75**, 1085 (2003).
[3] N. E. Hussey, K. Takenaka, and H. Takagi, Universality of the Mott–Ioffe–Regel limit in metals, Philos. Mag. **84**, 2847 (2004).
[4] H. Takagi, B. Batlogg, H. L. Kao, J. Kwo, R. J. Cava, J. J. Krajewski, and W. F. Peck, Systematic evolution of temperature-dependent resistivity in $La_{2-x}Sr_xCuO_4$, Phys. Rev. Lett. **69**, 2975 (1992).
[5] A. Tyler, A. Mackenzie, S. NishiZaki, and Y. Maeno, High temperature resistivity of Sr_2RuO_4: Bad metallic transport in a good metal, Phys. Rev. B **58**, R10107 (1998).
[6] Y. Kamihara, T. Watanabe, M. Hirano, and H. Hosono, Iron-based layered superconductor $La[O_{1-x}F_x]FeAs$ (x = 0.05–0.12) with $T_c = 26$ K, J. Am. Chem. Soc. **130**, 3296 (2008).
[7] Q. Si and E. Abrahams, Strong correlations and magnetic frustration in the high T_c iron pnictides, Phys. Rev. Lett. **101**, 076401 (2008).
[8] K. Takenaka, R. Shiozaki, and S. Sugai, Charge dynamics of a double-exchange ferromagnet $La_{1-x}Sr_xMnO_3$, Phys. Rev. B **65**, 184436 (2002).

[9] A. F. Hebard, T. T. M. Palstra, R. C. Haddon, and R. M. Fleming, Absence of saturation in the normal-state resistivity of thin films of K_3C_{60} and Rb_3C_{60}, Phys. Rev. B **48**, 9945 (1993).

[10] P. Limelette, P. Wzietek, S. Florens, A. Georges, T. A. Costi, C. Pasquier, D. Jérome, C. Mézière, and P. Batail, Mott transition and transport crossovers in the organic compound $\kappa-(\mathrm{BEDT-TTF})_2\mathrm{Cu}[\mathrm{N}(\mathrm{CN})_2]\mathrm{Cl}$, Phys. Rev. Lett. **91**, 016401 (2003).

[11] T. Valla, P. D. Johnson, Z. Yusof, B. Wells, Q. Li, S. M. Lourerio, R. J. Cava, M. Mikami, Y. Mori, M. Yoshimaru, and T. Sasaki, Coherence–incoherence and dimensional crossover in layered strongly correlated metals, Nature (London) **417**, 627 (2002).

[12] A. Damascelli, K. M. Shen, D. H. Lu, N. P. Armitage, F. Ronning, D. L. Feng, C. Kim, Z. X. Shen, T. Kimura, Y. Tokura, Z. Q. Mao, and Y. Maeno, Fermi surface of Sr_2RuO_4 from angle resolved photoemission, J. Electron Spectrosc. Relat. Phenom. **114–116**, 641 (2001).

[13] S. C. Wang, H. B. Yang, A. K. Sekharan, H. Ding, J. R. Engelbrecht, X. Dai, Z. Wang, A. Kaminski, T. Valla, T. Kidd, A. V. Fedorov, and P. D. Johnson, Quasiparticle line shape of Sr_2RuO_4 and its relation to anisotropic transport, Phys. Rev. Lett. **92**, 137002 (2004).

[14] T. Kondo, M. Ochi, M. Nakayama, H. Taniguchi, S. Akebi, K. Kuroda, M. Arita, S. Sakai, H. Namatame, M. Taniguchi, Y. Maeno, R. Arita, and S. Shin, Orbital-dependent band narrowing revealed in an extremely correlated Hund's metal emerging on the topmost layer of Sr_2RuO_4, Phys. Rev. Lett. **117**, 247001 (2016).

[15] M. Yi *et al.*, Observation of universal strong orbital-dependent correlation effects in iron chalcogenides, Nat. Commun. **6**, 7777 (2015).

[16] L. C. Rhodes, M. D. Watson, A. A. Haghighirad, M. Eschrig, and T. K. Kim, Strongly enhanced temperature dependence of the chemical potential in FeSe, Phys. Rev. B **95**, 195111 (2017).

[17] A. Mezio and R. H. McKenzie, Low quasiparticle coherence temperature in the one-band hubbard model: A slave-boson approach, Phys. Rev. B **96**, 035121 (2017).

[18] Th. Pruschke, D. L. Cox, and M. Jarrell, Hubbard model at infinite dimensions: Thermodynamic and transport properties, Phys. Rev. B **47**, 3553 (1993).

[19] J. Merino and R. H. McKenzie, Transport properties of strongly correlated metals: A dynamical mean-field approach, Phys. Rev. B **61**, 7996 (2000).

[20] N. Hussey, A. Mackenzie, J. Cooper, Y. Maeno, and S. Nishizaki, Normal-state magnetoresistance of Sr_2RuO_4, Phys. Rev. B **57**, 5505 (1998).

[21] X. Deng, J. Mravlje, R. Žitko, M. Ferrero, G. Kotliar, and A. Georges, How bad metals turn good: Spectroscopic signatures of resilient quasiparticles, Phys. Rev. Lett. **110**, 086401 (2013).

[22] W. Xu, K. Haule, and G. Kotliar, Hidden fermi liquid, scattering rate saturation, and nernst effect: A dynamical mean-field theory perspective, Phys. Rev. Lett. **111**, 036401 (2013).

[23] J. Mravlje, M. Aichhorn, T. Miyake, K. Haule, G. Kotliar, and A. Georges, Coherence-incoherence crossover and the mass-renormalization puzzles in Sr_2RuO_4, Phys. Rev. Lett. **106**, 096401 (2011).

[24] X. Deng, K. Haule, and G. Kotliar, Transport properties of metallic ruthenates: A DFT + DMFT investigation, Phys. Rev. Lett. **116**, 256401 (2016).

[25] F. B. Kugler, M. Zingl, H. U. Strand, S. S. B. Lee, J. Von Delft, and A. Georges, Strongly correlated materials from a numerical renormalization group perspective: How the Fermi-liquid state of Sr_2RuO_4 emerges, Phys. Rev. Lett. **124**, 016401 (2020).

[26] A. Tamai, M. Zingl, E. Rozbicki, E. Cappelli, S. Riccò, A. de la Torre, S. McKeown Walker, F. Y. Bruno, P. D. C. King, W. Meevasana, M. Shi, M. Radović, N. C. Plumb, A. S. Gibbs, A. P. Mackenzie, C. Berthod, H. U. R. Strand, M. Kim, A. Georges, and F. Baumberger, High-resolution photoemission on Sr_2RuO_4 reveals correlation-enhanced effective spin-orbit coupling and dominantly local self-energies, Phys. Rev. X **9**, 021048 (2019).

[27] A. P. Mackenzie, S. R. Julian, A. J. Diver, G. J. McMullan, M. P. Ray, G. G. Lonzarich, Y. Maeno, S. Nishizaki, and T. Fujita, Quantum oscillations in the layered perovskite superconductor Sr_2RuO_4, Phys. Rev. Lett. **76**, 3786 (1996).

[28] A. Damascelli, D. H. Lu, K. M. Shen, N. P. Armitage, F. Ronning, D. L. Feng, C. Kim, Z.-X. Shen, T. Kimura, Y. Tokura, Z. Q. Mao, and Y. Maeno, Fermi surface, surface states, and surface reconstruction in Sr_2RuO_4, Phys. Rev. Lett. **85**, 5194 (2000).

[29] Y. Maeno, K. Yoshida, H. Hashimoto, S. Nishizaki, S.-i. Ikeda, M. Nohara, T. Fujita, A. P. Mackenzie, N. E. Hussey, J. G. Bednorz, and F. Lichtenberg, Two-dimensional Fermi liquid behavior of the superconductor Sr_2RuO_4, J. Phys. Soc. Jpn. **66**, 1405 (1997).

[30] K. M. Shen, N. Kikugawa, C. Bergemann, L. Balicas, F. Baumberger, W. Meevasana, N. J. C. Ingle, Y. Maeno, Z.-X. Shen, and A. P. Mackenzie, Evolution of the Fermi surface and quasiparticle renormalization through a van hove singularity in $Sr_{2-y}La_yRuO_4$, Phys. Rev. Lett. **99**, 187001 (2007).

[31] See Supplemental Material at http://link.aps.org/supplemental/10.1103/PhysRevLett.131.236502, which includes Refs. [32–46], for experimental and theoretical methods, data analysis, and a discussion of the temperature evolution of Z in the half-filled single-orbital Hubbard model.

[32] M. Hoesch, T. Kim, P. Dudin, H. Wang, S. Scott, P. Harris, S. Patel, M. Matthews, D. Hawkins, S. Alcock, T. Richter, J. Mudd, M. Basham, L. Pratt, P. Leicester, E. Longhi, A. Tamai, and F. Baumberger, A facility for the analysis of the electronic structures of solids and their surfaces by synchrotron radiation photoelectron spectroscopy, Rev. Sci. Instrum. **88**, 013106 (2017).

[33] P. Blaha, K. Schwarz, G. Madsen, D. Kvasnicka, and J. Luitz, *WIEN2k, An Augmented Plane Wave+Local Orbitals Program for Calculating Crystal Properties* (K. Schwarz, Technische Universität Wien, Austria, 2001).

[34] N. Marzari and D. Vanderbilt, Maximally localized generalized Wannier functions for composite energy bands, Phys. Rev. B **56**, 12847 (1997).

[35] I. Souza, N. Marzari, and D. Vanderbilt, Maximally localized Wannier functions for entangled energy bands, Phys. Rev. B **65**, 035109 (2001).

[36] A. A. Mostofi, J. R. Yates, Y.-S. Lee, I. Souza, D. Vanderbilt, and N. Marzari, WANNIER90: A tool for obtaining maximally-localised Wannier functions, Comput. Phys. Commun. **178**, 685 (2008).

[37] O. Parcollet, M. Ferrero, T. Ayral, H. Hafermann, I. Krivenko, L. Messio, and P. Seth, TRIQS: A toolbox for research on interacting quantum systems, Comput. Phys. Commun. **196**, 398 (2015).

[38] M. Aichhorn, L. Pourovskii, P. Seth, V. Vildosola, M. Zingl, O. Peil, X. Deng, J. Mravlje, G. Kraberger, C. Martins, M. Ferrero, and O. Parcollet, TRIQS/DFTTools: A TRIQS application for *ab initio* calculations of correlated materials, Comput. Phys. Commun. **204**, 200 (2016).

[39] M. Kim, J. Mravlje, M. Ferrero, O. Parcollet, and A. Georges, Spin-orbit coupling and electronic correlations in Sr_2RuO_4, Phys. Rev. Lett. **120**, 126401 (2018).

[40] P. Seth, I. Krivenko, M. Ferrero, and O. Parcollet, TRIQS/CTHYB: A continuous-time quantum Monte Carlo hybridisation expansion solver for quantum impurity problems, Comput. Phys. Commun. **200**, 274 (2016).

[41] J. R. Yates, X. Wang, D. Vanderbilt, and I. Souza, Spectral and Fermi surface properties from Wannier interpolation, Phys. Rev. B **75**, 195121 (2007).

[42] O. Chmaissem, J. D. Jorgensen, H. Shaked, S. Ikeda, and Y. Maeno, Thermal expansion and compressibility of Sr_2RuO_4, Phys. Rev. B **57**, 5067 (1998).

[43] R. Bulla, T. A. Costi, and T. Pruschke, Numerical renormalization group method for quantum impurity systems, Rev. Mod. Phys. **80**, 395 (2008).

[44] R. Žitko and T. Pruschke, Energy resolution and discretization artifacts in the numerical renormalization group, Phys. Rev. B **79**, 085106 (2009).

[45] R. Zitko, NRG Ljubljana, 10.5281/zenodo.4841076 (2021).

[46] M. Zingl, J. Mravlje, M. Aichhorn, O. Parcollet, and A. Georges, Hall coefficient signals orbital differentiation in the Hund's metal Sr_2RuO_4, npj Quantum Mater. **4**, 35 (2019).

[47] C. Bergemann, A. P. Mackenzie, S. R. Julian, D. Forsythe, and E. Ohmichi, Quasi-two-dimensional Fermi liquid properties of the unconventional superconductor Sr_2RuO_4, Adv. Phys. **52**, 639 (2003).

[48] G. Levy, W. Nettke, B. M. Ludbrook, C. N. Veenstra, and A. Damascelli, Deconstruction of resolution effects in angle-resolved photoemission, Phys. Rev. B **90**, 045150 (2014).

[49] I. Osborne, T. Paiva, and N. Trivedi, Broken Luttinger theorem in the two-dimensional Fermi-Hubbard model, Phys. Rev. B **104**, 235122 (2021).

[50] R. S. Dhaka, S. E. Hahn, E. Razzoli, R. Jiang, M. Shi, B. N. Harmon, A. Thaler, S. L. Bud'ko, P. C. Canfield, and A. Kaminski, Unusual temperature dependence of band dispersion in $Ba(Fe_{1-x}Ru_x)_2As_2$ and its consequences for antiferromagnetic ordering, Phys. Rev. Lett. **110**, 067002 (2013).

[51] V. Brouet, P.-H. Lin, Y. Texier, J. Bobroff, A. Taleb-Ibrahimi, P. Le Fèvre, F. Bertran, M. Casula, P. Werner, S. Biermann, F. Rullier-Albenque, A. Forget, and D. Colson, Large temperature dependence of the number of carriers in co-doped $BaFe_2As_2$, Phys. Rev. Lett. **110**, 167002 (2013).

[52] J. A. N. Bruin, H. Sakai, R. S. Perry, and A. P. Mackenzie, Similarity of scattering rates in metals showing T-linear resistivity, Science **339**, 804 (2013).

[53] S. A. Hartnoll and A. P. Mackenzie, Colloquium: Planckian dissipation in metals, Rev. Mod. Phys. **94**, 041002 (2022).

[54] D. Abramovitch, J. Zhou, J. Mravlje, A. Georges, and M. Bernardi, Combining electron-phonon and dynamical mean-field theory calculations of correlated materials: Transport in the correlated metal Sr_2RuO_4, Phys. Rev. Mater. **7**, 093801 (2023).

[55] S. Kevan, *Angle-Resolved Photoemission: Theory and Current Applications*, Studies in Surface Science and Catalysis (Elsevier, New York, 1992).

[56] T. Miller, W. E. McMahon, and T.-C. Chiang, Interference between bulk and surface photoemission transitions in Ag(111), Phys. Rev. Lett. **77**, 1167 (1996).

[57] M. Thees, M.-H. Lee, R. L. Bouwmeester, P. H. Rezende-Gonçalves, E. David, A. Zimmers, F. Fortuna, E. Frantzeskakis, N. M. Vargas, Y. Kalcheim, P. L. Fèvre, K. Horiba, H. Kumigashira, S. Biermann, J. Trastoy, M. J. Rozenberg, I. K. Schuller, and A. F. Santander-Syro, Imaging the itinerant-to-localized transmutation of electrons across the metal-to-insulator transition in V_2O_3, Sci. Adv. **7**, eabj1164 (2021).

[58] M. Zonno *et al.*, Ubiquitous suppression of the nodal coherent spectral weight in bi-based cuprates, Phys. Rev. B **103**, 155109 (2021).

[59] https://doi.org/10.26037/yareta:ziluj4yuevexjc7u3v2ugvdx7e.